LAWRENCE
LIVERMORE
NATIONAL
LABORATORY

LLNL-JRNL-471954

Pressure-induced changes in the electronic structure of americium metal

P. Soderlind, K. T. Moore, A. Landa, J. A. Bradley

March 4, 2011

Physical Review B

Disclaimer

Pressure-induced changes in the electronic structure of americium metal

Per Söderlind, K. T. Moore, A. Landa, and J. A. Bradley

Lawrence Livermore National Laboratory,

Livermore, California 94550, USA

(Dated: February 24, 2011)

Abstract

We have conducted electronic-structure calculations for Am metal under pressure to investigate the behavior of the $5f$-electron states. Density-functional theory (DFT) does not reproduce the experimental photoemission spectra for the ground-state phase where the $5f$ electrons are localized, but the theory is expected to be correct when $5f$ delocalization occurs under pressure. The DFT prediction is that peak structures of the $5f$ valence band will merge closer to the Fermi level during compression indicating presence of itinerant $5f$ electrons. Existence of such $5f$ bands is argued to be a prerequisite for the phase transitions, particularly to the primitive orthorhombic AmIV phase, but does not agree with modern dynamical-mean-field theory (DMFT) results. Our DFT model further suggests insignificant changes of the $5f$ valence under pressure in agreement with recent resonant x-ray emission spectroscopy, but in contradiction to the DMFT predictions. The influence of pressure on the $5f$ valency in the actinides is discussed and is shown to depend in a non-trivial fashion on $5f$ band position and occupation relative to the *spd* valence bands.

PACS numbers: 71.15.Mb, 71.20.Gj,71.28.+d

I. INTRODUCTION

The actinide element series presents a wealth of interesting physical properties for metals, such as low-symmetry crystal structures, low thermal/electrical transport, and strongly anisotropic mechanical response.[1] One remarkable peculiarity is the large and abrupt change in atomic volume between plutonium and americium, which is nearly 50% between the neighboring elements in the periodic table. This large volume expansion is driven by the $5f$ electrons, which are bonding for Pu, but localized for Am.[2] The difference in $5f$ electron behavior between Pu and Am is clearly reflected by their ground-state crystal structures. α-Pu has a low-symmetry and openly-packed monoclinic structure, which is more typical of a mineral than a metal, while α-Am (or AmI) forms in a high-symmetry structure that is double-hexagonal close-packed (dhcp).

The smaller volume and more complex crystal structure of Pu relative to Am can be traced to the condition of the $5f$ electrons. In Pu the $5f$ electrons are bonding in narrow bands close to the highest occupied energy level (Fermi level, E_F). This causes the metal to distort through a Peierls-like symmetry-breaking mechanism.[3,4] This mechanism is only effective if there are many degenerate levels near the Fermi level, i.e., if the energy bands are narrow with a large electronic density of states (DOS). This is the case for the early actinides and particularly for α-Pu. The volume and crystal structure of Am, on the other hand, are consistent with bonding $6d$ electrons[5] with no significant influence from $5f$ electrons.

Americium metal has received considerable attention in the past and recently because of the unique changes in electronic and crystal structure that occur as functions of pressure.[6–14] At ambient conditions the $5f$ electrons are localized but with increasing pressure they begin to participate in bonding and delocalize. This change in character has a substantial effect on the equation-of-state as well as phase stability and transformations. The early reports concluded that Am went through transitions from its ground-state double hexagonal close-packed (dhcp) AmI phase to a face-centered-cubic (fcc) AmII, monoclinic AmIII, and eventually face-centered orthorhombic α-uranium-type AmIV.[6] The latter two assignments were questioned first by theory[8] and later determined to be face-centered and primitive orthorhombic, respectively.[9] Only the AmIII $\rightarrow$ AmIV showed[9] a significant volume collapse of 7%. These experimental findings[9] now have theoretical support from several DFT calculations.[12,15,16]

Because of the good agreement between the latest experimental work and DFT modeling with respect to phase stability in Am, one must conclude that the energetics is correctly described by the DFT approach. However, the exact nature of the $5f$ electrons during compression is still an open question. On issue is that DFT cannot accurately reproduce the non-magnetic atomic $5f^6$ configuration or the electronic spectra for AmI. This is shown in Fig. 1, which illustrates that both DMFT[13] and LDA+U[17] agree better with the experimental spectra[18] than our DFT treatment[12] at ambient pressure. However, in spite of failing to reproduce the non-magnetic structure or the electronic spectra, DFT does give a reasonable AmI energy relative to the other pressure-induced phases.

Few discussions have been focusing on the influence of pressure on the spectra of Am. DMFT[13] predicts the electronic density of states during compression to show a narrowing and lowering of unoccupied states and a broadening with peak structures about 2.5 eV and further below the Fermi level. Close and below (2 eV) E_F the DMFT DOS displays low intensity and no features at any compression. Such a DOS is inconsistent with the electronic-structure instability leading to distortions and existence of low-symmetry phases common in the actinides.[1,3] The interpretation of the DMFT DOS was an admixture of f^7 states with an increase of the $5f$ occupancy as a result. However, resonant x-ray emission spectroscopy[14] designed to confirm this DMFT prediction instead proved that the $5f$ valency remains unchanged during compression to 23 GPa, enough pressure to examine AmI through AmIV.

Our report discuss new DFT results of the DOS of Am and the changes that occur in $5f$-electron occupation under compression. TOut calculations show that the phase stability is correctly described by the density-functional-theory model, a fact that has been known for several years.[12,15,16] We also find that the main features of the electronic spectra at elevated pressure is predicted to have strong intensity in the vicinity ($\lesssim$ 1 eV) of the Fermi level (zero binding energy). This behavior of the spectra is required to account for the phase transitions that occur under compression. Finally, the $5f$ occupation is calculated within the DFT model and found to be essentially invariant under compression for americium. The lack of change in $5f$-electron occupation in Am with applied pressure is supported by resonant x-ray emission spectroscopy results,[14] but contradict DMFT results that propose an increase in $5f$ electrons due to pressure-induced admixture of a $5f^7$ configuration.[13] The present paper is organized as follows: Section II deals with computational technicalities,

Sect. III focuses on the ground-state AmI phase, followed by Sect. IV that includes the high-pressure phases. Because of the recent experimental study of $5f$ occupation[14] in Am, we devote one section to discuss more generally for actinides f-band occupation and how it is influenced by pressure in Sect. V. Lastly, we summarize and conclude in Sect. VI.

II. COMPUTATIONAL TECHNICALITIES

Most of the calculations presented here are conducted using an all-electron (no pseudopotential) technique implemented in the framework of density-functional theory. As dictated by DFT, the electron exchange and correlation energy functionals and associated potentials have to be assumed and we use the so-called generalized gradient approximation (GGA) for this purpose.[19] This implementation has proven to be robust for the actinides[20] and Am[12] notwithstanding the particular shortcomings of DFT to predict the spectral and magnetic properties of the ground-state of americium mentioned in the introduction.

The linear muffin-tin orbitals method does not constrain the shapes of the charge density or potential and the method is thus referred to as a full potential linear muffin-tin orbitals (FPLMTO) method.[21] Spin-orbit coupling (SO) is implemented in a first-order variational procedure[22] for the valence d and f states, as was done previously,[23] and for the core states the fully relativistic Dirac equation is solved. The inclusion of spin-orbit coupling for the $5f$ states of Am is important, since it has been experimentally shown to be strong.[24–26] The orbital polarization (OP) is accomplished as described in detail by Eriksson *et al.*[27] The energy of the orbitals with the spin, orbital, and magnetic quantum numbers (σ, l, m_l) are shifted an amount proportional to $L_\sigma m_l$. Here L_σ is the total orbital moment from electrons with spin σ. This self-consistent parameter-free technique attempts to generalize Hund's second rule for an atom to the condensed matter and enhances the separation of the m_l orbitals caused by the spin-orbit interaction. Hence, the orbital polarization can be viewed as an amplification of the SO. Most of the details of the present calculations are similar to those given earlier for Am.[12]

In the discussions of orbital projected (s, p, d, or f) states we employ calculations with the atomic-sphere-approximation (ASA) as well as so-called exact muffin-tin orbitals (EMTO) method[28] that includes SO.[29] The former is also utilized to calculate band edges by means of properties of the so-called logarithmic-derivative functions that are related to the potential

functions that are defined in the ASA method.[30] One advantage of these techniques, albeit less accurate for energy calculations, is that the projected occupation numbers are unique while for the full-potential methods they will depend on the size of the chosen muffin-tin sphere.

III. THE GROUND-STATE PHASE

We first consider the energetics and equation-of-state for Am comparing theory and experiment. In Fig. 2 we show the calculated equation-of-states for AmI and AmII with the experimental data of Heathman *et al.*[9] Our calculations predict AmI and AmII to be energetically close to degenerate, as pointed out earlier.[12] In reality AmI should have a somewhat lower total energy, since it is the observed ground-state phase. The agreement with experiment is rather good although theory overestimate slightly the equilibrium volumes (close to 30 Å^3 versus 29.3 Å^3). The bulk moduli are in good agreement as well with theoretical values of 26 GPa versus $\sim$ 30 GPa in the measurements.[9]

The ground-state spectral and magnetic properties are not correctly described within the DFT model. The localized $5f$ electrons in AmI occupy an atomic $5f^6$ state with a $J = 0$ non-magnetic configuration. The DFT model, on the other hand, predicts large spin polarization of delocalized $5f$ electrons essentially representing energetically the true localized $5f^6$ configuration,[31] but with incorrect spectra and magnetic properties. In Fig. 1 we compare our DFT DOS with that of DMFT,[13] LDA+U,[17] and experimental data.[18] Most of the DFT intensity lies within 2 eV of the Fermi level whereas experimentally it has a broad feature from 1 to 5 eV below the Fermi level.[18] The LDA+U[17] and DMFT[13] models are in some disagreement with the data,[18] but are more realistic than the DFT model, with substantial density of states in the -2 to -4 eV range. The $5f$ states are thus withdrawn from the Fermi level and pose little importance for the chemical bonding, equation-of-state, and crystal structure. Instead, it is clear that the $6d$ states play the major role[5] for these properties in AmI. During compression, however, the $5f$ orbitals are forced to overlap more and with this delocalization process increase their influence on the cohesive properties in the high-pressure phases.

IV. PRESSURE-INDUCED PHASES

Pressure induces a series of phase transitions in Am. The ambient-pressure dhcp structure of AmI first transforms to face-centered cubic (fcc) AmII at about 6 GPa. The structure then transforms to face-centered orthorhombic (fco) AmIII at 10 GPa, followed by the primitive orthorhombic (po) AmIV at 16 GPa.[9] Except for the AmI-AmII transformation, DFT calculations reproduce these phase changes extremely well and also predict a body-centered-cubic phase (AmV) to ultimately become stable.[12] We show the energy differences relative to AmI (α-Am) for these phases in Fig. 3 that we have compiled from the data published previously.[12]

It has been argued for some time, as we mention in the introduction, that typical actinide phases such as orthorhombic (α-U, α-Np, AmIV) are stabilized by a Peierls-like symmetry-breaking mechanism that acts upon narrow $5f$ bands positioned at the Fermi level.[3] For example, AmIV is stable over AmII because the band energy is lower in AmIV due to less occupied states at higher energy levels compared to AmII, see Fig. 4. The figure clearly illustrates that substantial weight of the DOS is removed from E_F in AmIV opening up a deep valley at the highest occupied energy that lowers the energy in comparison to the distribution of states found in AmII. It is unquestionable that the $5f$ electrons are delocalized at the pressures where AmIV is stable, since the low-symmetry crystal structure give clear evidence of $5f$ bonding. Further affirmation is given by a canonical band model with itinerant f electrons, which shows that precisely AmIV is favored over other plausible phases for f occupations corresponding to Am.[32] Another hint that full delocalization has occurred for AmIV is the fact that the magnetic moments are all suppressed at this pressure in the calculations. Any remaining $5f$-localization in Am would have manifested itself through spin polarization in the DFT treatment as a necessary but not sufficient condition.

Localized $5f$ states are not involved in determining the crystal structure. Nor can they support distortions to lower symmetry phases because such states have different spectra with intensities at lower binding energies removed from E_F, as is the case for AmI in Fig. 1. The AmIV phase is quite different in this regard. From the calculated AmIV DOS we can simulate a photoemission spectra by first truncating with the Fermi-Dirac function (T=100 K) and then apply instrumental and lifetime broadening as suggested by Arko *et al.*[33] The result, in Fig. 5, displays a spectra for AmIV with a broad peak and maximum intensity at about

-0.8 eV consistent with delocalized $5f$ electrons. On the contrary, DMFT calculations[13] for Am corresponding to the volume of the AmIV phase (they use a face-centered-cubic unit cell at the volume of AmIV rather than the actual primitive orthorhombic unit cell) produce a localized $5f$-electron picture with intensity several eV below the Fermi level removing the possibility of actually stabilizing AmIV. These DMFT calculations also propose an increase of the $5f$ valency due to an admixture of $5f^7$ states, which we discuss in the next section.

V. $5f$ OCCUPATION IN ACTINIDES UNDER PRESSURE

In the early actinides, the $5f$-band occupation increases with pressure mainly because the kinetic energy contribution is larger for orbitals with more nodes (number of nodes $= n - l - 1$) as discussed by McMahan and Albers for the late $3d$ transition metal Ni.[34] In Fig. 6 we show calculated (ASA) band centers for uranium illustrating that $7s$ and $7p$ indeed increase in energy more rapidly than $6d$ and $5f$, which increases at the lowest rate. Fig. 6 is most relevant for electron occupations close to half filled (center of the band), but in reality the actual occupation of a specific state is important. Anti-bonding states will rise in energy more rapidly with compression than bonding states and this is obvious in Fig. 7 that shows results obtained from ASA calculations of uranium. Here, anti-bonding $5f$ states (close to the upper edge of the $5f$ band) are rising faster than bonding $6d$ states (close to the lower edge of the $6d$ band). Accordingly, this effect suggests that compression will cause a transfer from the $5f$ to the other bands for heavier actinides, thus reducing the $5f$-band occupation. Combining these two mechanisms proposes that early actinides with available bonding $5f$ states will populate these states at the expense of the other orbital states. On the other hand, the opposite will occur for the later actinides, which have filled anti-bonding $5f$ states. Somewhere in the middle one expects these two effects to compete with each other, resulting in a nearly invariant $5f$-band population as a function of compression.

Literature has shown that phase transitions in Ce, Th, and Pa are due to pressure-induced increase of f electrons.[35,36] In the case of Pa, this means approaching uranium in the periodic table of elements and consequently Pa adopts the α-U phase under compression. Few discussions of the change of $5f$ valency with pressure for the remaining actinides can be found except for the aforementioned DMFT work that states an increase with pressure for Am.[13]

We compile calculated (FPLMTO) $5f$ occupation-changes with compression in Fig. 8 for Pa-Bk. Th is omitted, since it is practically identical to Pa. The figure clearly shows that the early actinides Pa, U, and Np increase their f population rapidly as the volume is reduced with pressure. On the other hand, Pu, Am, and Cm, which are closer to the middle of the f band, show rather weak dependence. For Bk, the midpoint of the f band is passed and the metal loses electrons with compression. This is in good accord with the trends expected from the arguments put forward in the previous paragraphs. As already alluded to in Sect. II, the FPLMTO method cannot define the occupation numbers uniquely because of the need to specify a muffin-tin sphere volume in which the electrons can be projected onto orbitals. Consequently, Fig. 8 is somewhat skewed because a small amount of $5f$ electrons will leave the muffin-tin sphere under compression and are therefore not counted. This accounting problem is small and not important for most actinides except those with nearly invariant $5f$-band occupation. Therefore we also conduct, for Am, EMTO calculations that do not have this bookkeeping issue in Fig. 9. In this plot we can also compare the difference between various phases of Am metal. AmII and AmIV behave similarly with a change of the $5f$ valency that is never greater than about 0.04, which is a very small fraction (0.6%) of the total $5f$ occupation in the calculation (6.4). Furthermore, at the onset of AmIV at $\sim 40\%$ compression, the change in occupation number is approaching zero.

Our DFT predictions of $5f$ electron occupation and valency in Am as a function of pressure differ from recent DMFT calculations.[13] DMFT actually predicts formation of magnetic moments through an admixture of an f^7 configuration with a very large total moment of $J = 7/2$ that is screened by valence *spd* electrons. On the contrary, our DFT results clearly show nearly no change in the $5f$ valency with pressure. This DFT prediction is supported by resonant x-ray emission spectroscopy results that show the $5f$ valency remains unchanged during compression.[14] Thus, while DMFT appears to be suited for the ground-state phase of Am, it is not consistent with the general understanding of $5f$-electron behavior in the actinides under compression.

VI. CONCLUSION

Three fundamental properties of americium under pressure are discussed. First, phase stability is correctly described by the density-functional-theory model, a fact that has been

known for a few years already.[12,15,16] Second, the main features of the electronic spectra at elevated pressure is predicted to have strong intensity in the vicinity ($\lesssim 1$ eV) of the Fermi level (zero binding energy). This behavior of the spectra is required to account for the several phase transitions that occur under compression and is completely opposite of that predicted by DMFT calculations.[13] Thirdly, the $5f$ occupation or valency is calculated within the DFT model and found to be essentially invariant under compression for americium. This is so because there is a balance between (i) anti-bonding $5f$ electrons, that want to expand the lattice, are lost to the other s, p, and d states during compression and (ii) transfer of *spd* valence electrons to the $5f$ band due to kinetic-energy effects during compression. The lack of change in $5f$electron occupation in Am with applied pressure has been supported by resonant x-ray emission spectroscopy results, which also show no change during compression.[14] The insignificant pressure dependence of the $5f$ valency suggested by the DFT calculations thus agrees with experiment,[14] but is in contradiction with the DMFT results that propose an increase in $5f$ electrons due to pressure-induced admixture of a $5f^7$ configuration.

The issue of $5f$ electron occupation and valency in actinide materials is of great importance. We see this here, where it is intrinsically tied to the electronic, magnetic and crystal structure of Am metal as a function of pressure. With this in mind, the electron valence must be experimentally investigated for Am as a function of pressure. The typical measurement to understand these properties is x-ray photoemission spectroscopy. However, the technique uses a low primary energy that can not penetrate the diamond-anvil cells needed to achieve high pressure. For this reason, other techniques must be employed that have a high primary energy adequate to penetrate the diamonds or gasket. Resonant x-ray emission spectroscopy can be utilized at high pressure,[37] and this and has already been employed for Am as discussed above.[14] Another option is non-resonant x-ray emission spectroscopy (NRIXS), which has been used on actinide materials at ambient conditions to examine electron valence.[38] The primary energy of this technique is $\sim$ 10 keV, meaning it can penetrate a perforated diamond anvil cell and be used to examine either the $O_{4,5}$ edge ($5d \rightarrow 5f$) near 100 eV or the $N_{4,5}$ ($4d \rightarrow 5f$) edge near 800 eV. Furthermore, the technique is bulk sensitive,[39] which means impurity phases near the sample surface due to preparation will be less of an issue for highly reactive actinide materials.[40] High-pressure NRIXS work is under progress and will surely illuminate how pressure influences $5f$ electron occupation near the itinerant-localized transition in the actinide series.

Acknowledgments

J. G. Tobin and R. G. Haire are acknowledged for helpful discussions. This work performed under the auspices of the U.S. Department of Energy by Lawrence Livermore National Laboratory under Contract DE-AC52-07NA27344.

---

[1] K. T. Moore and G. van der Laan, Rev. Mod. Phys. **81**, 235 (2009).

[2] E. A. Kmetko and H. H. Hill, *Plutonium 1970 and Other Actinides*, edited by W. N. Miner (AIME, New York, 1970), p. 233.

[3] P. Söderlind, O. Eriksson, B. Johansson, J. M. Wills, and A. M. Boring, Nature **374**, 524 (1995).

[4] In a one-dimensional lattice, a Peierls distortion allows a row of equidistant atoms to lower its total energy by forming pairs. The lower periodicity causes the degenerate energy levels to split into two bands with lower and higher energies. The electrons occupy the lower levels, so that the distortion increases the bonding and reduces the total energy. In one-dimensional systems, the distortion opens an energy gap at the Fermi level making the system an insulator. However, in the higher dimensional systems the material remains a metal after the distortion because other Bloch states fill the gap.

[5] J. C. Duthie and D. G. Pettifor, Phys. Rev. Lett. **38**, 564 (1977); A. K. McMahan, H. L. Skriver, and B. Johansson, Phys. Rev. B **23**, 5016 (1981).

[6] R. B. Roof, R. G. Haire, D. Schiferl, L. A. Schwalbe, E. A. Kmetko, and J. L. Smith, Science **207**, 1353 (1980).

[7] P. Link, D. Braithwaite, J. Wittig, U. Benedict, and R. G. Haire, J. Alloys Compd. **213**, 148 (1994).

[8] P. Söderlind, R. Ahuja, O. Eriksson, B. Johansson, and J. M. Wills, Phys. Rev. B **61**, 8119 (2000).

[9] S. Heathman, R. G. Haire, T. Le Bihanm A. Lindbaum, K. Litfin, Y. Meresse, and H. Libotte, Phys. Rev. Lett. **85**, 2961 (2000).

[10] A. Lindbaum, S. Heathman, K. Litfin, Y. Meresse, R. G. Haire, T. Le Bihan, and H. Libotte, Phys. Rev. B **63**, 214101 (2001).

[11] J. -C. Griveau, J. Rebizant, G. H. Lander, G. Kotliar, Phys. Rev. Lett. **94**, 097002 (2005).

[12] P. Söderlind and A. Landa, Phys. Rev. B **72**, 024109 (2005).

[13] S. Y. Savrasov, K. Haule, and G. Kotliar, Phys. Rev. Lett. **96**, 036404 (2006).

[14] S. Heathman, J. -P. Rueff, L. Simonelli, M. A. Denecke, J. -C. Griveau, R. Caciuffo, and G. H. Lander, Phys. Rev. B **82**, 201103 (2010).

[15] M. Pénicaud, J. Phys.: Condens. Matter **14**, 3575 (2002).

[16] M. Pénicaud, J. Phys.: Condens. Matter **17**, 257 (2005).

[17] M. F. Islam and A. K. Ray, Sol. State. Comm. **150**, 938 (2010).

[18] T. Gouder, P. M. Oppeneer, F. Huber, F. Wastin, and J. Rebizant, Phys. Rev. B **72**, 115122 (2005).

[19] J. P. Perdew, J. A. Chevary, S. H. Vosko, K. A. Jackson, M. R. Pederson, D. J. Singh, and C. Fiolhais, Phys. Rev. B **46**, 6671 (1992).

[20] P. Söderlind, Adv. Phys. **47**, 959 (1998).

[21] J. M. Wills, O. Eriksson, M. Alouani, and D. L. Price, in *Electronic Structure and Physical Properties of Solids*, edited by H. Dreysse (Springer-Verlag, Berlin, 1998), p. 148.

[22] O. K. Andersen, Phys. Rev. B **12**, 3060 (1975).

[23] L. Nordström, J. M. Wills, P. H. Andersson, P. Söderlind, and O. Eriksson, Phys. Rev. B **63**, 035103 (2000).

[24] K. T. Moore, G. van der Laan, R. G. Haire, M. A. Wall, A. J. Schwartz, and P. Söderlind, Phys. Rev. Lett. **98**, 236402 (2007)

[25] K. T. Moore, G. van der Laan, M. A. Wall, A. J. Schwartz, and R. G. Haire, Phys. Rev. B **76**, 073105 (2007)

[26] M. T. Butterfield, K. T. Moore, G. van der Laan, M. A. Wall, and R. G. Haire, Phys. Rev. B **77**, 113109 (2008)

[27] O. Eriksson, M. S. S. Brooks, and B. Johansson, Phys. Rev. B **41**, 9087 (1990).

[28] L. Vitos, *Computational Quantum Mechanics for Materials Engineers: The EMTO Method and Applications* (Springer, London, 2007).

[29] L. V. Pourovskii, A. V. Ruban, L. Vitos, H. Ebert, B. Johansson, and I. A. Abrikosov, Phys. Rev. B **71**, 094415 (2005).

[30] H. L. Skriver, *The LMTO Method* (Springer-Verlag, Berlin, 1984).

[31] H. L. Skriver, O. K. Andersen, and B. Johansson, Phys. Rev. Lett. **44**, 1230 (1980).

[32] J. G. Tobin, P. Söderlind, A. Landa, K. T. Moore, A. J. Schwartz, B. W. Chung, M. A. Wall,

J. M. Wills, R. G. Haire, A. L. Kutepov, J. Phys.: Condens. Matter **20**, 125204 (2008).

[33] A. J. Arko, J. J. Joyce, L. Morales, J. Wills, J. Lashley, F. Wastin, and J. Rebizant, Phys. Rev. B **62**, 1773 (2000).

[34] A. K. McMahan and R. C. Albers, Phys. Rev. Lett. **49**, 1198 (1982).

[35] P. Söderlind, O. Eriksson, B. Johansson, and J. M. Wills, Phys. Rev. B **52**, 13169 (1995).

[36] P. Söderlind and O. Eriksson, Phys. Rev. B **56**, 10719 (1997).

[37] J. -P. Rueff and A. Shukla, Rev. Mod. Phys. **82**, 847 (2010).

[38] J. A. Bradley, S. Sen Gupta, G. T. Seidler, K. T. Moore, M. W. Haverkort, G. A. Sawatzky, S. D. Conradson, D. L. Clark, S. A. Kozimor, and K. S. Boland, Phys. Rev. B **81**, 193104 (2010).

[39] R. A. Gordon, G. T. Seidler, T. T. Fister, M. W. Haverkort, G. A. Sawatzky, A. Tanaka and T. K. Sham, EPL **81**, 26004 (2008).

[40] K. T. Moore, Micron **41**, 336 (2010).

Figures

FIG. 1: (Color online). Theoretical electronic density of states for AmI obtained from DMFT[13] (red), LDA+U[17], (blue) and present DFT calculations. Experimental photoemission spectra is from Gouder *et al.*[18] Zero binding energy corresponds to the Fermi level.

FIG. 2: Calculated (FPLMTO) results for equation-of-states of AmI and AmII. The horizontal line indicates zero pressure. Experimental data are from Heathman *et al.*[9]

FIG. 3: (Color online). FPLMTO energy differences, relative to AmI for AmII through AmV. The data are compiled from Söderlind and Landa.[12]

FIG. 4: (Color online). Calculated (FPLMTO) electronic density of states for AmII (red, dashed line) and AmIV at about 40% compression. The vertical line indicates the Fermi level.

FIG. 5: Simulated photoemission spectra for AmIV at about 40% compression. The spectra is obtained from applying instrumental and lifetime broadening[33] to the calculated density of state that has also been truncated with the Fermi-Dirac function (T=100 K). Zero binding energy corresponds to the Fermi level.

FIG. 6: (Color online). Calculated (ASA) band-center energy change as a function of compression for uranium metal. All band centers are shifted to zero at the equilibrium volume (V_0). The $5f$ band center rises slowest which suggests a pressure-induced increase of $5f$ population.

FIG. 7: (Color online). Calculated (ASA) $6d$ (red) and $5f$ band edges as a function of compression for uranium metal. Notice that the upper $5f$ band edge has a greater slope than the lower $6d$ band edge.

FIG. 8: (Color online). Calculated (FPLMTO) $5f$-band occupation change as functions of compression for Pa-Bk in a hypothetical face-centered-cubic phase.

FIG. 9: Calculated (EMTO) $5f$-band occupation change as functions of compression for AmII and AmIV.

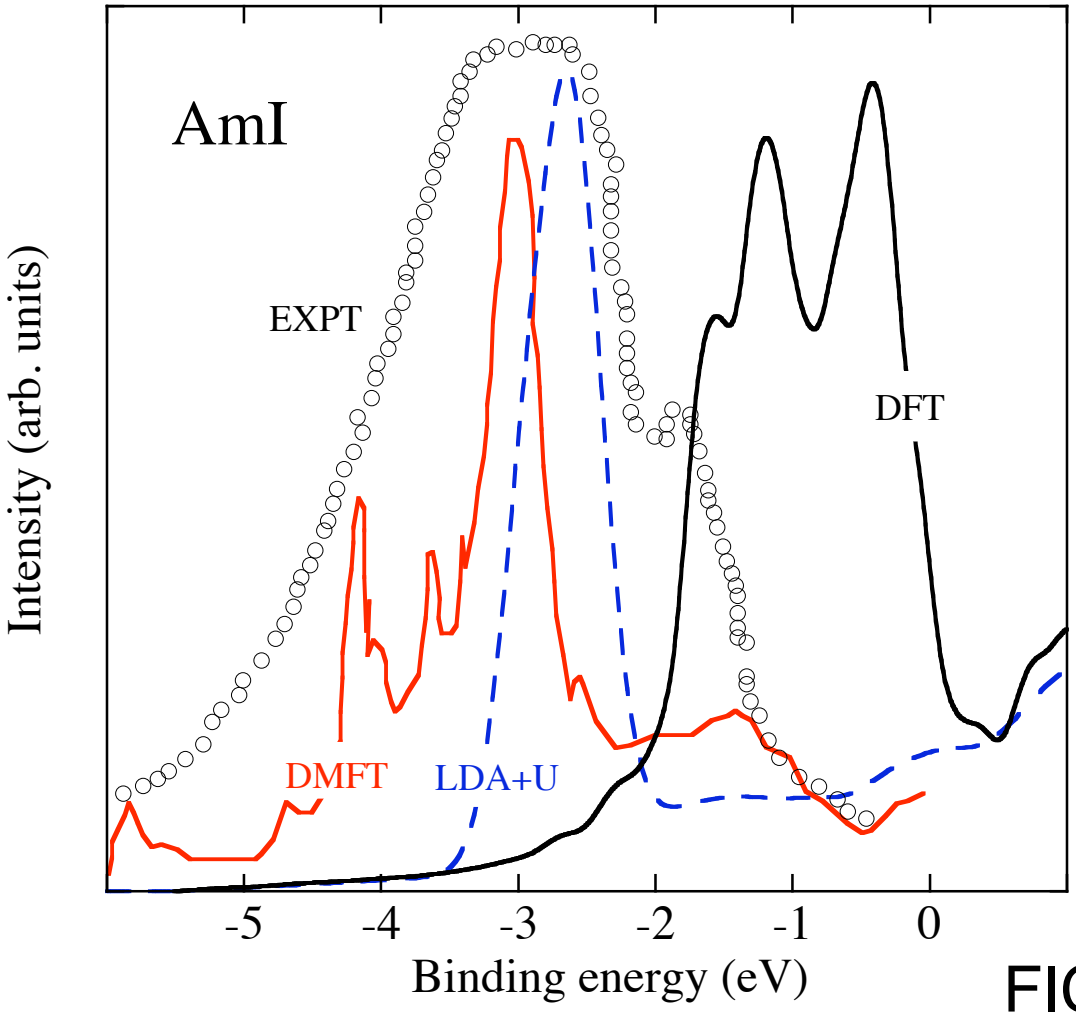
AmI
EXPT
DFT
DMFT
LDA+U
Intensity (arb. units)
-5
-4
-3
-2
-1
0
Binding energy (eV)

FIG. 1

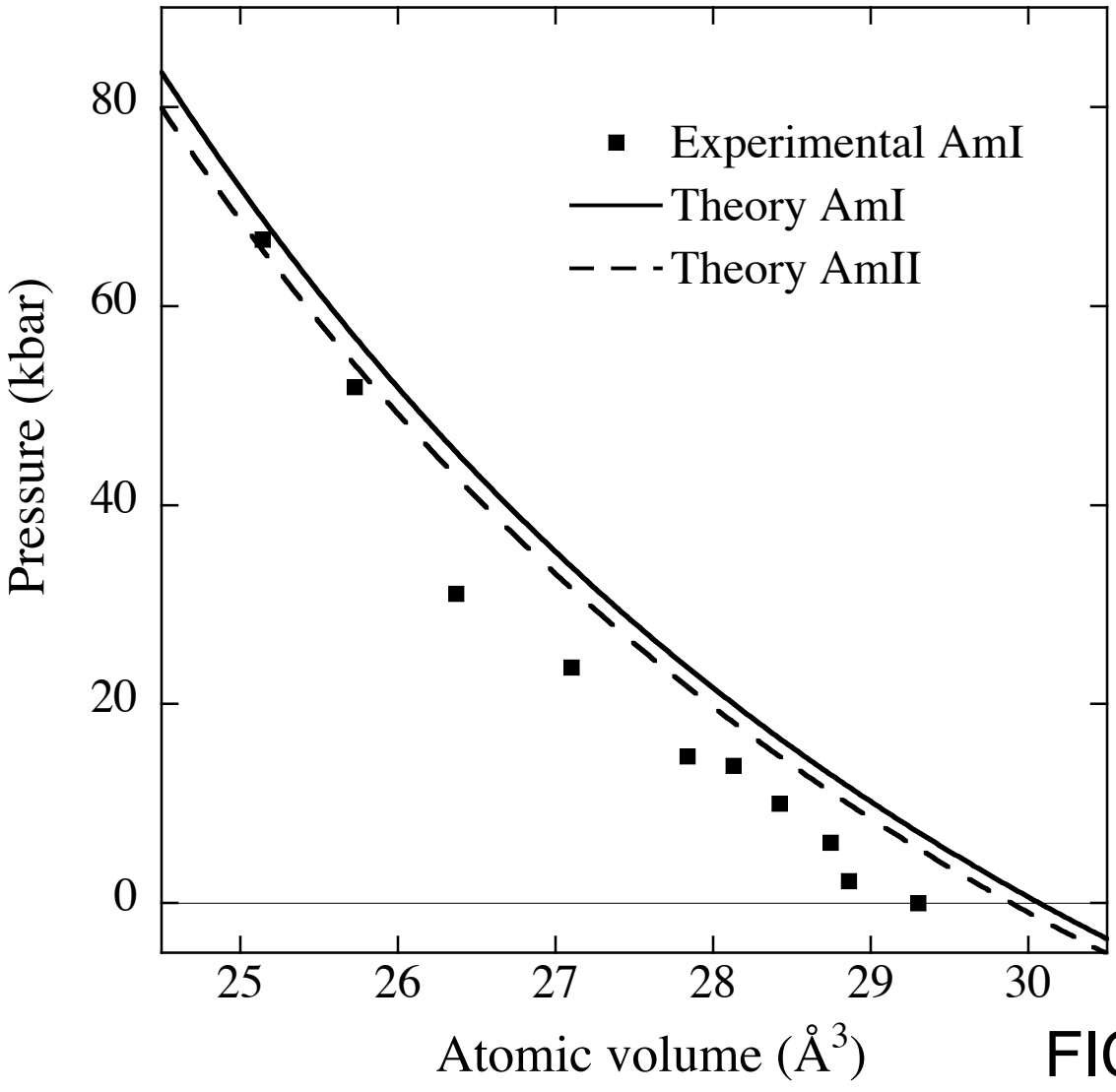
Experimental AmI
Theory AmI
Theory AmII
Pressure (kbar)
80
60
40
20
0
25
26
27
28
29
30
Atomic volume (Å^3)

FIG. 2

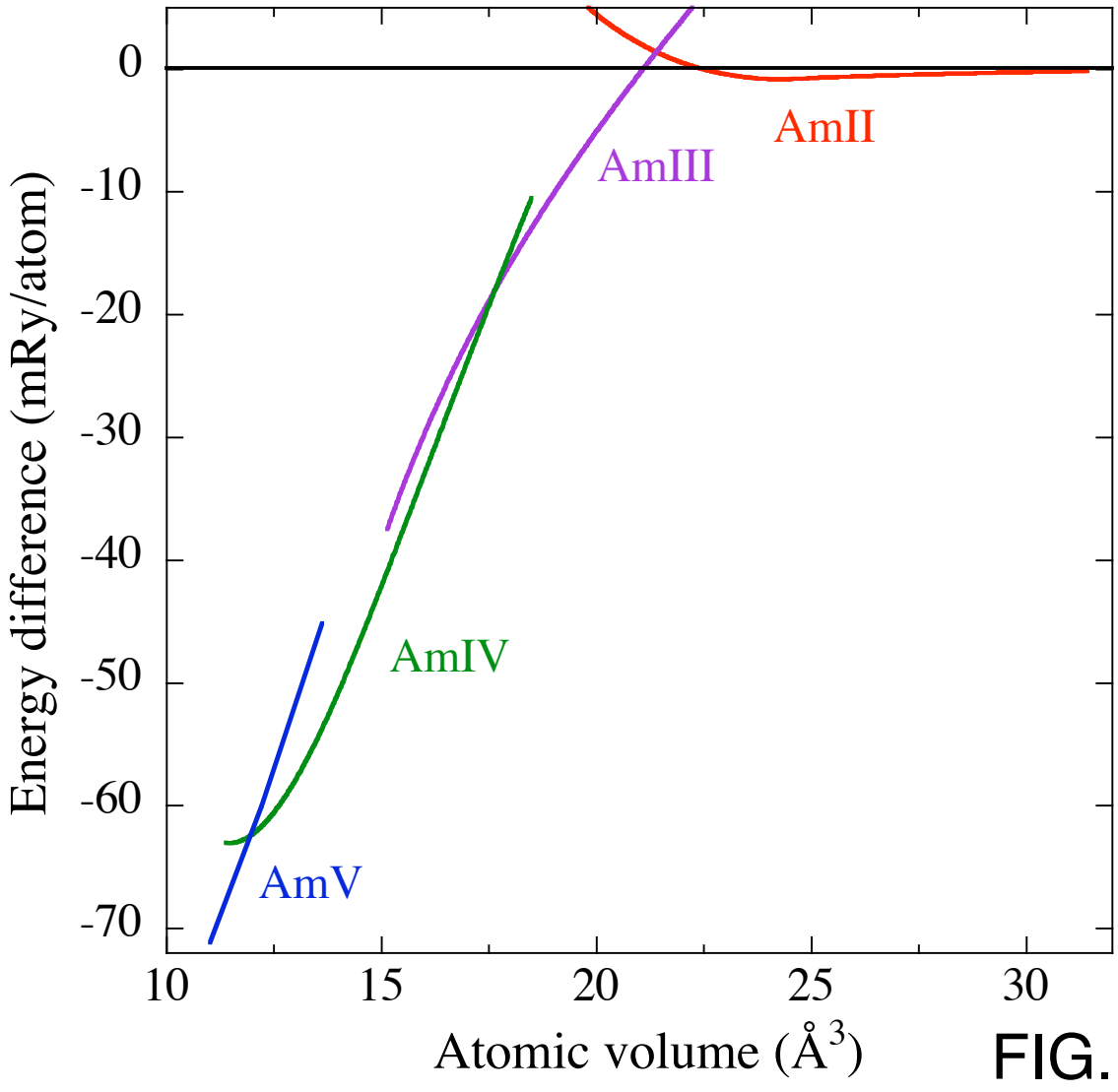
0
-10
-20
-30
-40
-50
-60
-70
Energy difference (mRy/atom)
10
15
20
25
30
Atomic volume (Å^3)
AmII
AmIII
AmIV
AmV

FIG. 3

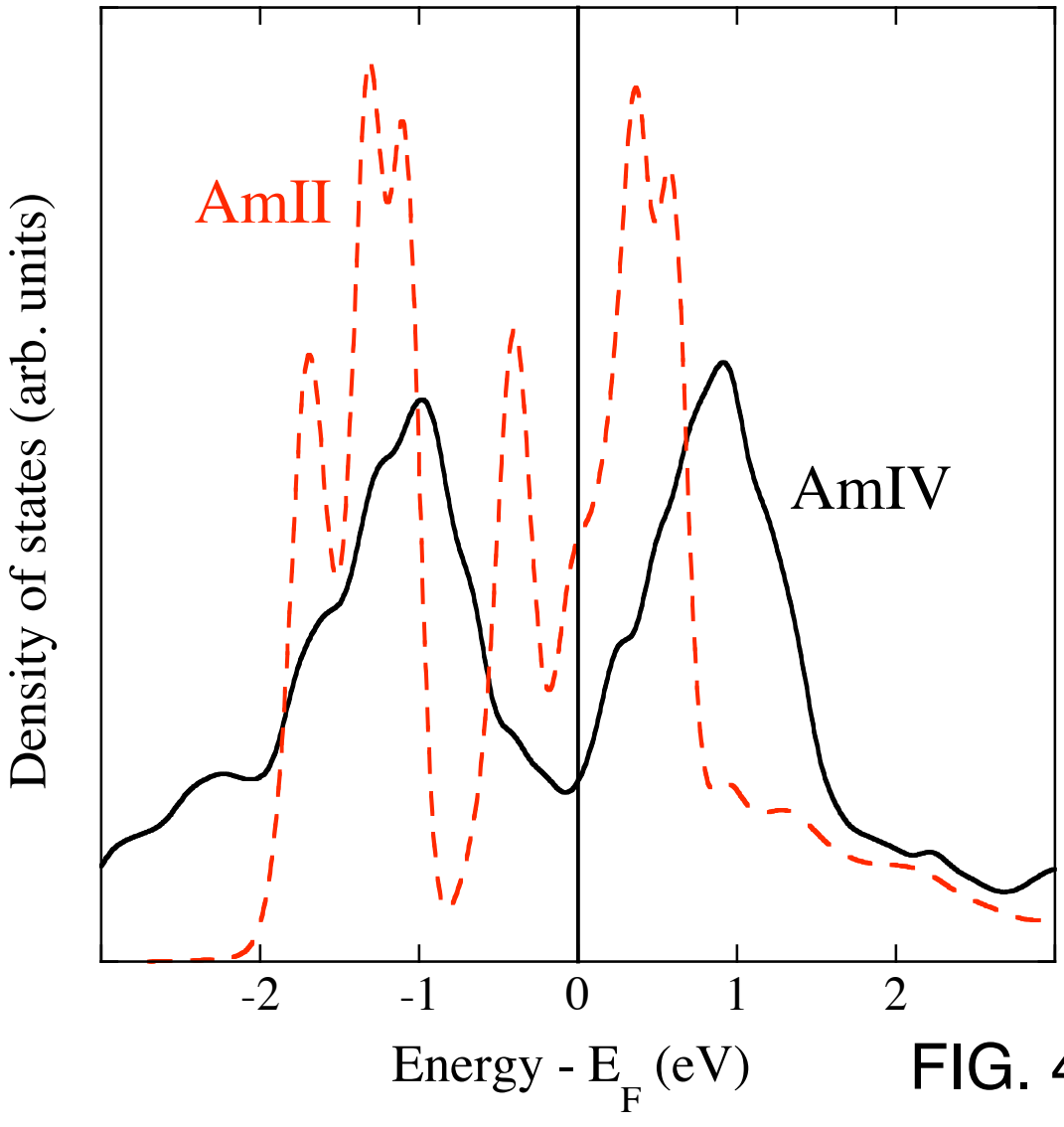

FIG. 4

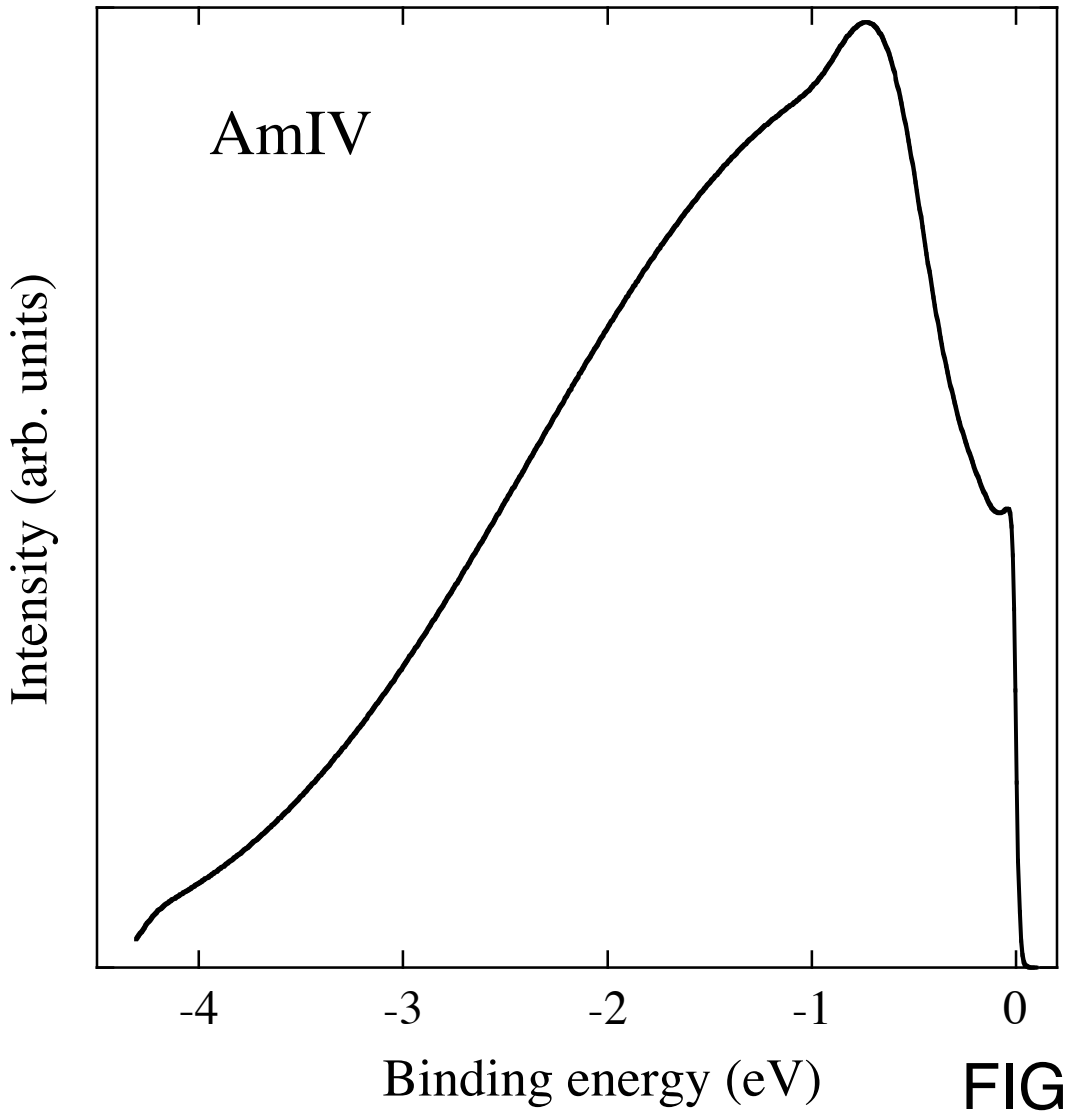

FIG. 5

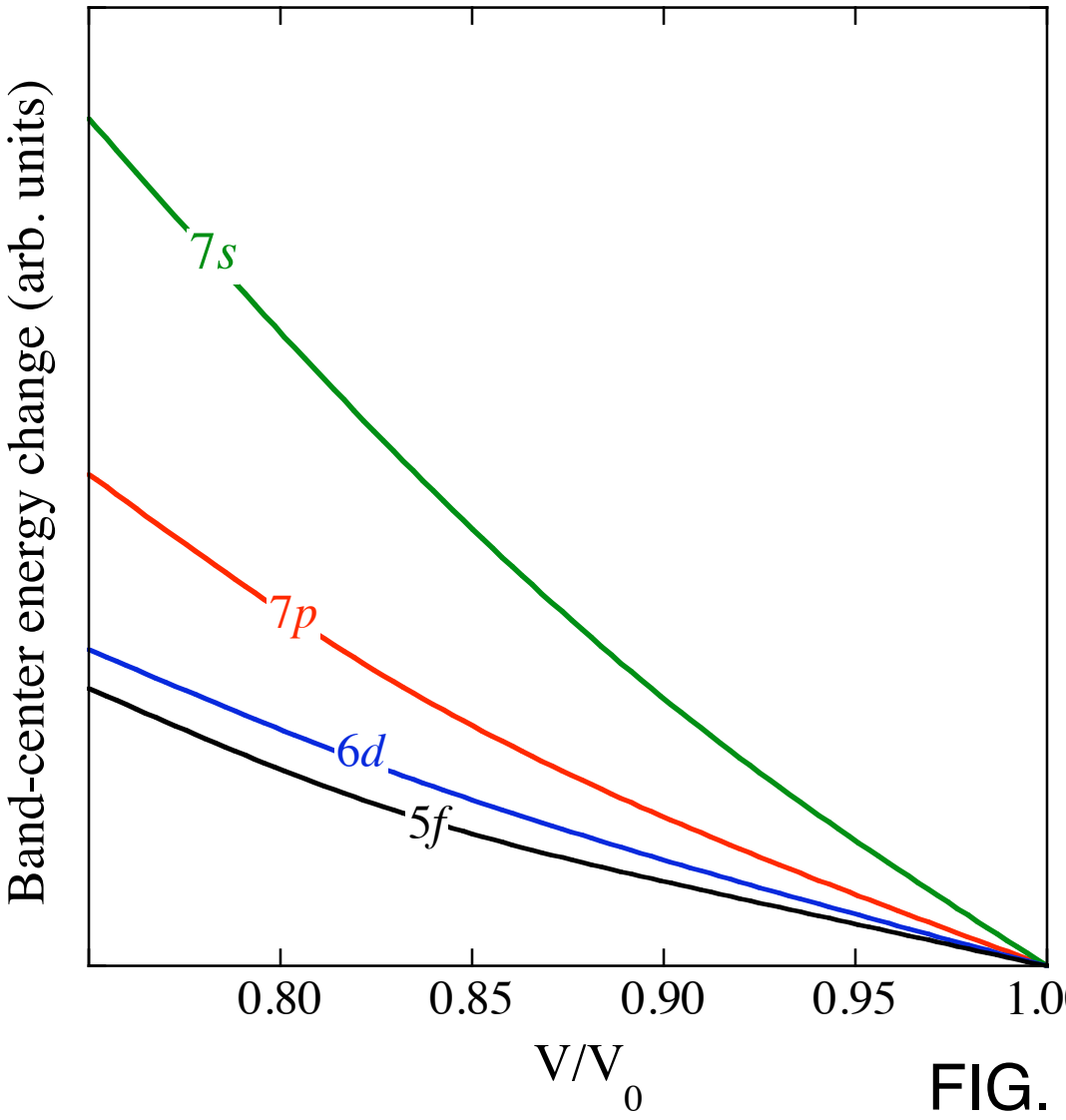
Band-center energy change (arb. units)
7s
7p
6d
5f
0.80
0.85
0.90
0.95
1.00
V/V0

FIG. 6

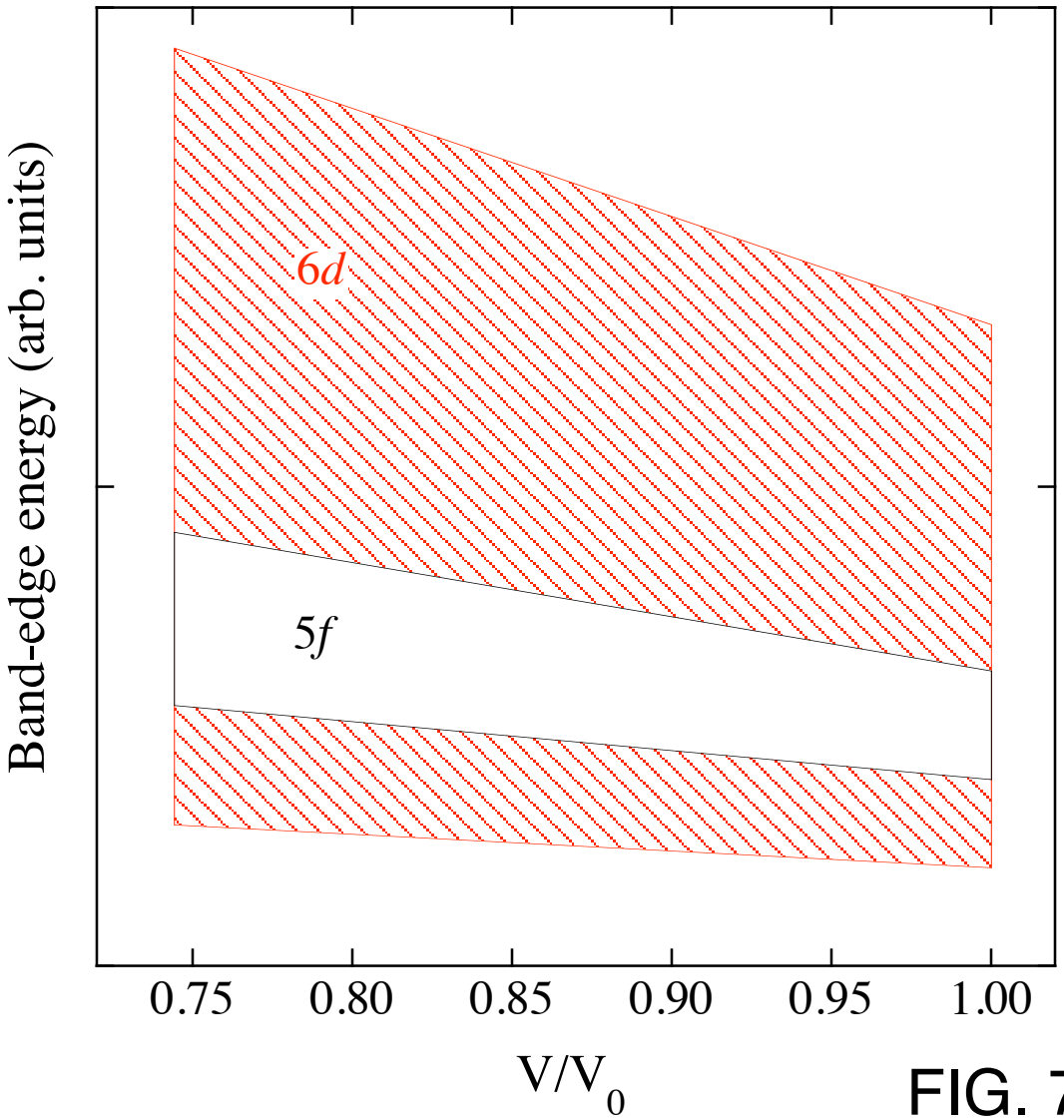

FIG. 7

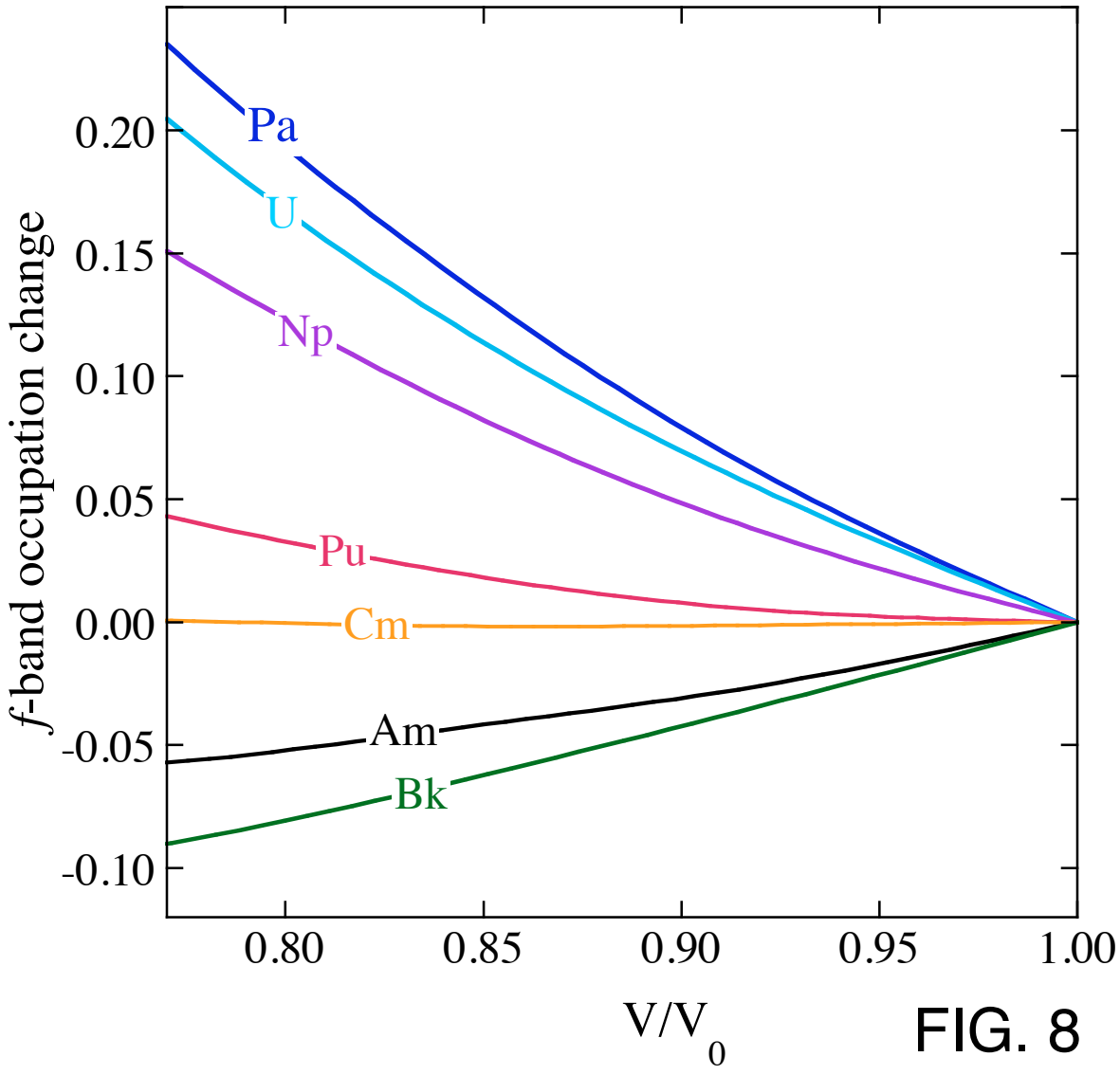
Pa
U
Np
Pu
Cm
Am
Bk
0.20
0.15
0.10
0.05
0.00
-0.05
-0.10
0.80
0.85
0.90
0.95
1.00
f-band occupation change
V/V0

FIG. 8

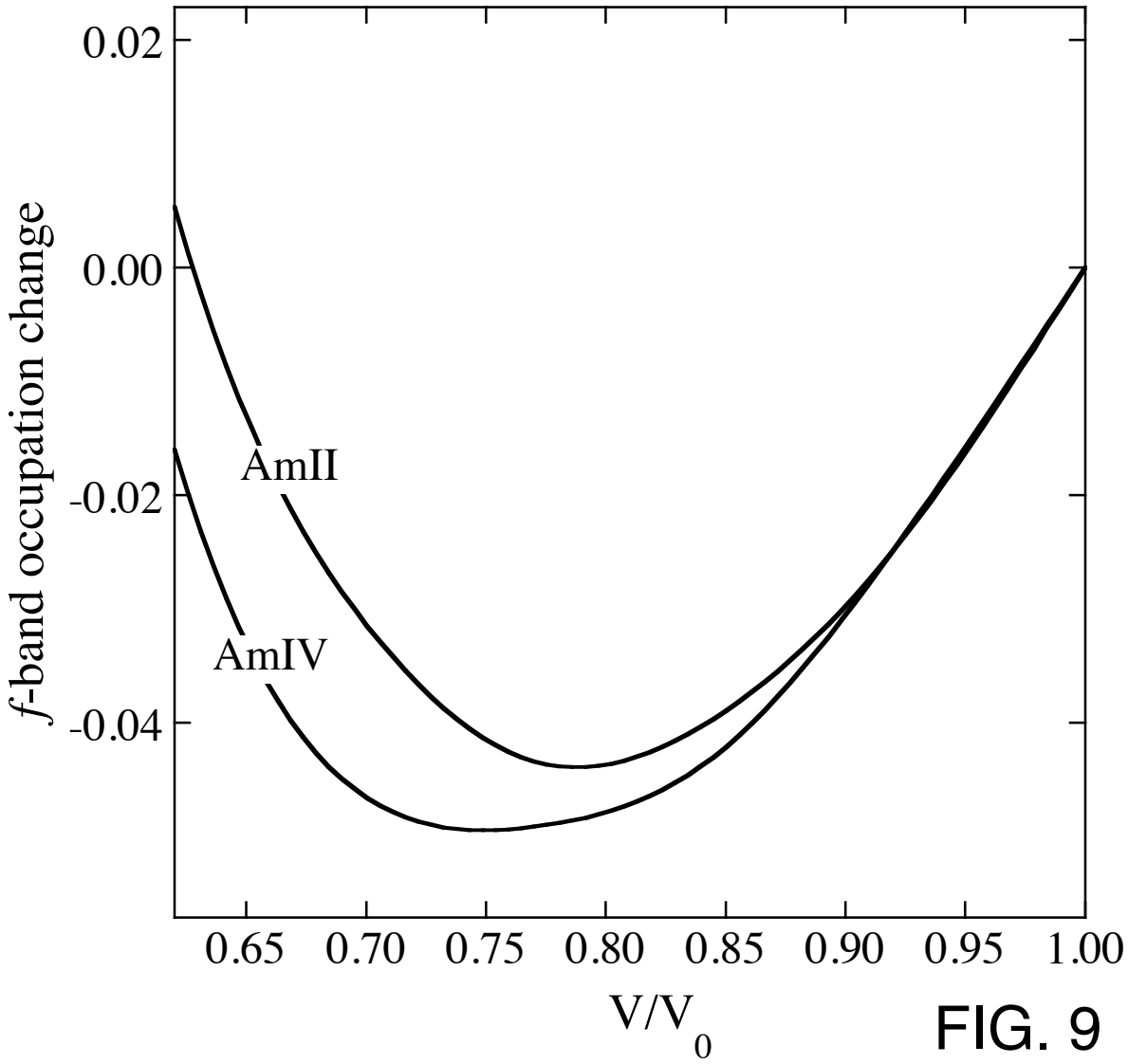
0.02
0.00
-0.02
-0.04
f-band occupation change
AmII
AmIV
0.65
0.70
0.75
0.80
0.85
0.90
0.95
1.00
V/V0

FIG. 9